Femtochemistry in Ionic Liquids

DOI: 10.1002/anie.200906046

12′-Apo-β-caroten-12′-al: An Ultrafast "Spy" Molecule for Probing Local Interactions in Ionic Liquids**

Kawon Oum, Peter W. Lohse, Florian Ehlers, Mirko Scholz, Matthäus Kopczynski, and Thomas Lenzer**

Ionic liquids (ILs), which consist exclusively of ions, are one of the current challenges for experimental investigations and theoretical modeling in chemistry. Knowledge of the microscopic interactions in ILs is required to predict their properties and design task-specific ILs for applications in fields such as synthesis, (bio)catalysis, and electrochemistry.[1–4] Surprisingly, attempts to characterize interactions between ILs and solute molecules by powerful techniques based on ultrafast spectroscopy have been fairly sparse.[5,6] Such information is however crucial, because the local environment of a molecule in the IL determines its dynamics and chemical reactivity.

Herein we characterize the solvation processes and polarity of ILs by employing the carbonyl carotenoid 12′-apo-β-caroten-12′-al (12′C)[7–11] as a probe for ultrafast pump–supercontinuum-probe (PSCP) broadband absorption spectroscopy.[14–16] We first focus on the dynamics of the electronically excited states of 12′C, with intramolecular charge-transfer character in the energetically lowest one ("S_1/ICT").[9,10,12,13] Figure 1 shows PSCP spectra of 12′C in $[C_4mim]^+[Tf_2N]^-$ upon excitation to the S_2 state at 480 nm. At early times (upper panel), negative $S_0 \rightarrow S_2$ ground-state bleaching (GSB) and $S_2 \rightarrow S_0$ stimulated emission (SE) are observed. Superimposed Raman structure of 12′C appears mainly on the anti-Stokes side. At the same time, transient excited state absorption (ESA, $S_2 \rightarrow S_n$) appears between 500 and 770 nm.

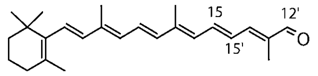

12'C

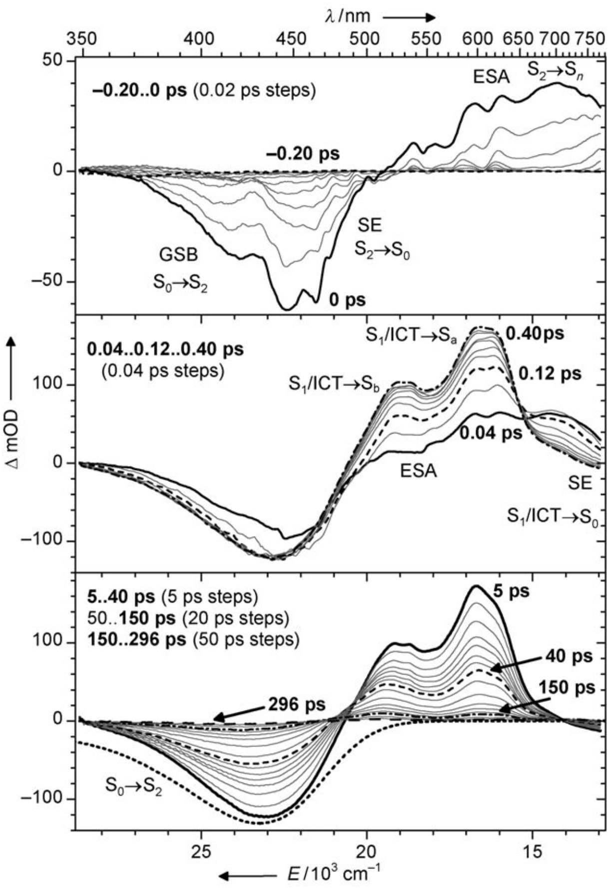

Figure 1. Transient PSCP absorption spectra of 12′C in $[C_4mim]^+[Tf_2N]^-$ for excitation at 480 nm. ΔmOD = change in optical density (×10^{-3}).

In the middle panel of Figure 1, a fast internal conversion (IC) from S_2 to S_1/ICT is visible ($\tau_2 = 130$ fs), which is characterized by the decay of the SE and ESA features of S_2 and the concomitant increase of a characteristic double-peak ESA band (610 and 530 nm) owing to transitions from S_1/ICT to two higher-lying electronic states (denoted in the following as S_a and S_b). There is no "clean" isosbestic point visible at about 650 nm, which suggests additional superimposed dynamics and is first evidence for solvation by the IL. The weak SE above 700 nm is a unique signature of ICT character of such probes.[7–13]

---

[*] Priv.-Doz. Dr. K. Oum, Dipl.-Chem. P. W. Lohse,
Dipl.-Chem. F. Ehlers, M. Scholz, Dipl.-Chem. M. Kopczynski,
Priv.-Doz. Dr. T. Lenzer
Institut für Physikalische Chemie
Georg-August-Universität Göttingen
Tammannstrasse 6, 37077 Göttingen (Germany)
Fax: (+49) 551-39-3150
E-mail: koum@gwdg.de
tlenzer@gwdg.de

[**] We thank N. P. Ernsting and J. L. Pérez-Lustres (Humboldt-Universität Berlin) for generous support during the implementation of the Pump-Supercontinuum Probe (PSCP) setup and H. Ernst (BASF AG) for providing the highly purified carotenoid sample. This work was supported by the German Research Foundation (DFG) priority programme SPP 1191.

Supporting information for this article, including details of the pump–supercontinuum probe (PSCP) broadband transient absorption setup, the near-IR transient absorption experiment, and global analysis of the transient spectra and the 12′C and IL samples, is available on the WWW under http://dx.doi.org/10.1002/anie.200906046.

On a longer timescale (Figure 1, bottom panel), the depopulation of the S_1/ICT state to S_0 is observed: The $S_1/\text{ICT}\rightarrow S_a,S_b$ ESA bands and the $S_1/\text{ICT}\rightarrow S_0$ SE feature decay and the S_0 GSB is filled up (see also for comparison the inverted $S_0\rightarrow S_2$ steady-state absorption spectrum). The persistent blue-shift in the S_1/ICT band region is due to solvation dynamics of the IL, and it is visible on the $S_1/\text{ICT}\rightarrow S_b$ ESA band and in the 430 nm region of the GSB. The latter indicates that an additional $S_1/\text{ICT}\rightarrow S_c$ ESA band is superimposed on the GSB. We also observe that the ESA peak ratio (610/530 nm) decreases with time, which is related to solvation.

Key points of the dynamics crucial to the solvent response and polarity of ILs shall now be discussed. A global analysis of the PSCP spectra was performed based on the kinetic scheme $S_2\rightarrow S_1/\text{ICT}\rightarrow S_0$ by considering time-dependent solvation of the dipolar S_1/ICT state (see Table 1 and the Supporting Information). Spectra are depicted in Figure 2 for 12′C in $[\text{C}_4\text{mim}]^+[\text{Tf}_2\text{N}]^-$ (top), methanol (middle), and THF (bottom). The qualitatively similar spectral development for $[\text{C}_4\text{mim}]^+[\text{Tf}_2\text{N}]^-$ and methanol takes place on different timescales. A pronounced blue-shift is obvious, especially for the $S_1/\text{ICT}\rightarrow S_b,S_c$ ESA transitions. The SE contribution in the near IR is relatively weak and overlapped by strong ESA, but the global analysis suggests that it shifts further to the red with increasing time until it coincides with the inverted steady-state fluorescence spectrum (dot-dash line for methanol). Such spectral dynamics are typical for solvent relaxation around a dipolar CT state.[17] The varying shifts of the individual ESA transitions must be due to the different electronic character of the terminal states: The clear blue-shifts for the S_b and S_c transitions suggest smaller dipole moments, but obviously a similar one for the S_a state (the most-red feature). The amplitudes of the S_a and S_b features become similar as solvent relaxation proceeds, which can be due to changes in the Franck–Condon factors and/or redistribution of population on the complex S_1/ICT potential energy surface along the relaxation pathway.

Table 1: Summary of global analysis.[a]

Solvent	τ_{fast} [ps]	τ_{slow} [ps]	τ_2 [ps]	τ_1 [ps]
$[\text{C}_4\text{mim}]^+[\text{Tf}_2\text{N}]^-$	0.65	29 ($\beta=0.82$)	0.13	44
$[\text{C}_4\text{mmim}]^+[\text{Tf}_2\text{N}]^-$	1.9	32 ($\beta=0.79$)	0.13	55
methanol	0.12, 0.99	11.9	0.12	6.4
THF	0.228, 1.52	–	0.14	80
n-hexane	–	–	0.10	192

[a] For abbreviations and further details, see the Supporting Information.

The presence of solvent relaxation is further underlined in THF, which is known to exhibit fast dynamics.[18] In this case, the spectral development is basically complete after 5 ps. In contrast, solvation in methanol also covers longer timescales (e.g., 0.12, 0.99, and 11.9 ps).[19] The spectral development in $[\text{C}_4\text{mim}]^+[\text{Tf}_2\text{N}]^-$ is described best by an ultrafast exponential response ($\tau_{\text{fast}}=0.65$ ps) and a second slow stretched-exponential component[5] ($\tau_{\text{slow}}=29$ ps, $\beta=0.82$). For the C2-methylated analogue $[\text{C}_4\text{mmim}]^+[\text{Tf}_2\text{N}]^-$, slightly larger values are found (Table 1). Furthermore, transient absorption profiles at 860 nm in other ILs were recorded (see Supporting Information). Our global analysis procedure showed that at this wavelength, the build-up of SE is particularly sensitive to the ultrafast component of solvation, and τ_{fast} values of between 0.5 and 1.8 ps were obtained, which is in good agreement with the PSCP results.

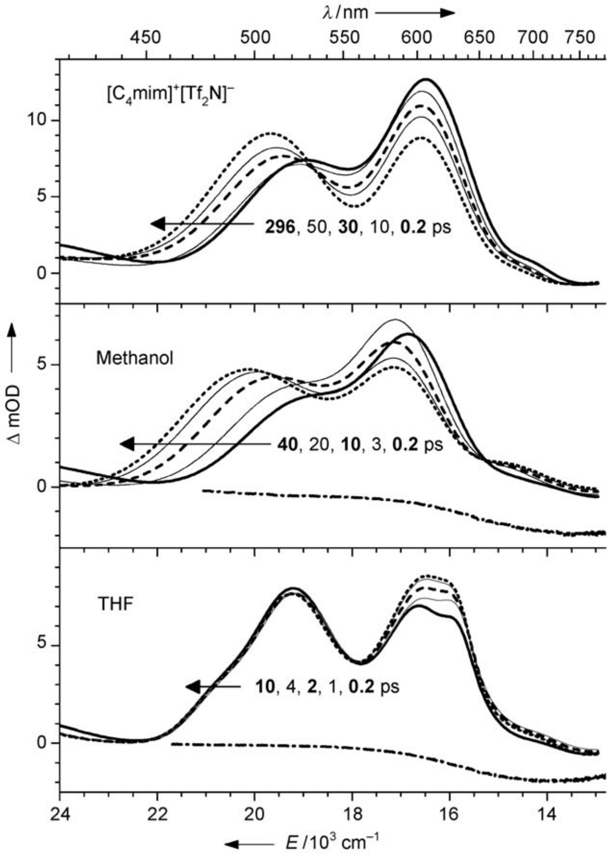

Figure 2. Time-dependent spectra for the S_1/ICT state of 12′C from global analysis in $[\text{C}_4\text{mim}]^+[\text{Tf}_2\text{N}]^-$ (top), methanol (middle), and THF (bottom).

The ultrafast process may be due to inertial translation of ions, with typical distances of < 100 pm during τ_{fast} in the case of ILs.[5] The slower response most likely involves cage deformation and reformation processes.[5,6] We can also compare our results with recent studies for several imidazolium-based ILs from optical Kerr effect (OKE) spectroscopy, dielectric relaxation spectroscopy (DRS), and time-domain terahertz and far-infrared FTIR spectroscopy in the 200 MHz–10 THz range.[20–24] The spectra are relatively broad and consist of overlapping solvent modes. The resulting IL response encompasses time components in the range 80 fs–5 ns, which is in accord with our ultrafast experiments.

The pronounced solvent-induced ESA blue-shift in $[\text{C}_4\text{mim}]^+[\text{Tf}_2\text{N}]^-$ deserves further comment. Its size is slightly smaller than in methanol, and much bigger than for THF and other non H-bonding solvents that were screened. For molecules such as 4-aminophthalimide, substantial differences of this kind are usually explained by specific solute–solvent interactions that are predominantly due to different hydrogen-bonding networks of the two electronic states involved in the transition.[17,25] It is tempting to assign the shift for $[C_4mim]^+[Tf_2N]^-$ also to H-bonds, which have been suggested to play an important role in ILs.[26] However, we find essentially the same shift for the C-2-methylated analogue $[C_4mmim]^+[Tf_2N]^-$, where H-bonding is largely suppressed. We therefore suggest that the spectral shift is due to specific probe–ion interactions, presumably between cations and the carbonyl group of 12′C, which results in stabilization of the S_1/ICT dipole. Such a view is compatible with our previous study[7] and the substantial cation-related Stokes shifts found for alkaline salt solutions in non H-bonding solvents.[27]

Information on the polarity of ILs can be obtained from the S_1/ICT lifetime τ_1 (Table 1). In organic solvents, we observe a strong polarity dependence: 192 ps (*n*-hexane) > 80 ps (THF) > 6.4 ps (methanol). For the two ILs, values fall into the range between methanol and THF; that is, the polarity experienced by the 12′C probe is comparable to that of short-chain alcohols. A similar trend can be found upon plotting the transient PSCP spectra for each solvent at $t=\tau_1$ (Figure 3). The amplitude ratio of the two bands can then be used as an empirical polarity parameter: 0.24 in *n*-hexane, 1.13 in THF and 1.62 in methanol. ILs such as $[C_4mim]^+$-$[Tf_2N]^-$ show an intermediate behavior (1.43), suggesting a polarity between THF and methanol, confirming the trend of the lifetimes (see Supporting Information for further discussion).

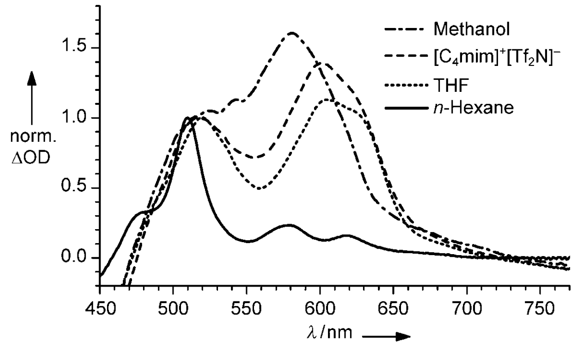

Figure 3. Dependence of the S_1/ICT ESA band shape on solvent polarity compared at $t=\tau_1$ of each solvent. The spectra were normalized at the left peak.

In summary, we have shown that 12′C can be employed as an ultrafast probe for ILs: Time-dependent shifts of the S_1/ICT band report on solvation dynamics, revealing a sub-picosecond component, which should be due to inertial translation of ions, and a second slower component owing to complex cage deformation and reformation processes on broadly distributed timescales. The time-dependent blue-shifts of the S_1/ICT band in ILs are dominated by specific probe–cation interactions. The unique lifetime dependence of the S_1/ICT state shows that 12′C experiences a polarity comparable to short-chain alcohols. In future investigations, we will employ different members of this probe molecule class that provide access to longer timescales, and we will also measure time-dependent Stokes shifts of other probes to further characterize IL relaxation processes.

Received: October 27, 2009

Keywords: carotenoids · femtochemistry · ionic liquids · laser spectroscopy · time-resolved spectroscopy

---

[1] H. Weingärtner, *Angew. Chem.* **2008**, *120*, 664; *Angew. Chem. Int. Ed.* **2008**, *47*, 654.
[2] P. Wasserscheid, T. Welton, *Ionic Liquids in Synthesis*, 2nd ed., Wiley-VCH, Weinheim, **2007**.
[3] F. Endres, S. Zein El Abedin, *Phys. Chem. Chem. Phys.* **2006**, *8*, 2101.
[4] A. A. H. Pádua, M. F. C. Gomes, J. N. C. Lopes, *Acc. Chem. Res.* **2007**, *40*, 1087.
[5] S. Arzhantsev, J. Hui, G. A. Baker, M. Maroncelli, *J. Phys. Chem. B* **2007**, *111*, 4978.
[6] A. Samanta, *J. Phys. Chem. B* **2006**, *110*, 13704.
[7] P. W. Lohse, R. Bürsing, T. Lenzer, K. Oum, *J. Phys. Chem. B* **2008**, *112*, 3048.
[8] F. Ehlers, T. Lenzer, K. Oum, *J. Phys. Chem. B* **2008**, *112*, 16690.
[9] M. Kopczynski, F. Ehlers, T. Lenzer, K. Oum, *J. Phys. Chem. A* **2007**, *111*, 5370.
[10] F. Ehlers, D. A. Wild, T. Lenzer, K. Oum, *J. Phys. Chem. A* **2007**, *111*, 2257.
[11] D. A. Wild, K. Winkler, S. Stalke, K. Oum, T. Lenzer, *Phys. Chem. Chem. Phys.* **2006**, *8*, 2499.
[12] J. A. Bautista, R. E. Connors, B. B. Raju, R. G. Hiller, F. P. Sharples, D. Gosztola, M. R. Wasielewski, H. A. Frank, *J. Phys. Chem. A* **1999**, *103*, 8751.
[13] D. Zigmantas, T. Polívka, R. G. Hiller, A. Yartsev, V. Sundström, *J. Phys. Chem. A* **2001**, *105*, 10296.
[14] T. Lenzer, S. Schubert, F. Ehlers, P. W. Lohse, M. Scholz, K. Oum, *Arch. Biochem. Biophys.* **2009**, *483*, 213.
[15] J. L. Pérez Lustres, S. A. Kovalenko, M. Mosquera, T. Senyushkina, W. Flasche, N. P. Ernsting, *Angew. Chem.* **2005**, *117*, 5779; *Angew. Chem. Int. Ed.* **2005**, *44*, 5635.
[16] S. A. Kovalenko, A. L. Dobryakov, J. Ruthmann, N. P. Ernsting, *Phys. Rev. A* **1999**, *59*, 2369.
[17] M. Sajadi, T. Obernhuber, S. A. Kovalenko, M. Mosquera, B. Dick, N. P. Ernsting, *J. Phys. Chem. A* **2009**, *113*, 44.
[18] M. L. Horng, J. A. Gardecki, A. Papazyan, M. Maroncelli, *J. Phys. Chem.* **1995**, *99*, 17311.
[19] A. L. Dobryakov, S. A. Kovalenko, N. P. Ernsting, *J. Chem. Phys.* **2005**, *123*, 044502.
[20] D. A. Turton, J. Hunger, A. Stoppa, G. Hefter, A. Thoman, M. Walther, R. Buchner, K. Wynne, *J. Am. Chem. Soc.* **2009**, *131*, 11140.
[21] C. Wakai, A. Oleinikova, M. Ott, H. Weingärtner, *J. Phys. Chem. B* **2005**, *109*, 17028.
[22] H. Weingärtner, *Z. Phys. Chem.* **2006**, *220*, 1395.
[23] H. Weingärtner, P. Sasisanker, C. Daguenet, P. J. Dyson, I. Krossing, J. M. Slattery, T. Schubert, *J. Phys. Chem. B* **2007**, *111*, 4775.
[24] J. Hunger, A. Stoppa, R. Buchner, G. Hefter, *J. Phys. Chem. B* **2009**, *113*, 9527.
[25] E. Krystkowiak, K. Dobek, A. Maciejewski, *J. Photochem. Photobiol. A* **2006**, *184*, 250.
[26] K. Fumino, A. Wulf, R. Ludwig, *Angew. Chem.* **2008**, *120*, 8859; *Angew. Chem. Int. Ed.* **2008**, *47*, 8731.
[27] C. F. Chapman, M. Maroncelli, *J. Phys. Chem.* **1991**, *95*, 9095.